Modelling and Control of PMSG Based Offshore Wind Turbine

Joan Francesc Quetglas Villalonga
joan.villalonga@tecnico.ulisboa.pt
Instituto Superior Técnico, Universidade de Lisboa, Portugal
September 2022

***Abstract*—The aim of this project is to model a wind turbine driven by permanent magnetic synchronous generator (PMSG) and to design the control of the WT able to support and recover from voltage sags. Moreover, this project demonstrates the efficiency and the effects of a voltage sag on the grid stability and the robustness of the voltage source converter (VSC) as converter in the WT world.**

The generator side inverter, adjusts the synchronous generator and decouples it from the grid when necessary, for example when the voltage sags occurs. On the other hand, the grid-side inverter oversees the power flow between the DC bus and the AC side. Moreover the fault-ride through capability has the capability to recover fast after a fault clearance. The simulation results in Matlab Simulink 2021b shows that the model has good dynamics and it recovers with a short time after a voltage drop, stabilizing the turbine.

***Index Terms*—Voltage Source Converter, Fault Ride Through, Wind Power, PMSG**

I. Introduction

Worldwide demands and energy consumption are rapidly increasing because of the exponential growth of the population, technology modernization and industrialization. This rapid growth has required different technologies to be applied in different countries in order to increase the electrification rate. Distributed energy resources (DERs) are being incorporated to the utility grid as a common method due to various reasons: low maintenance requirements, economic, cost saving and environmental impact.

Even onshore wind power is still the key player in the wind industry (707.396 MW by the end of 2020) offshore wind power is rapidly gaining importance in the future of the renewable energies in Europe [1] and it will be a key player in the next years as the share of renewable energies increases leaving the major production weight to the colossal wind turbines to be installed in the seas. By the end of 2020 a total of 35.196 MW had been installed.

Due to this full-scale voltage source converters (VSC) has appeared as key elements to integrate RE into the grid [2], [3] improving the efficiency of the sources as well ensuring the grid health and capability. Nowadays, VSC is not only used in the renewable energy (RE) generation interconnection but also energy storage systems (ESS) to boost the capacity factor of RE generation.

The objectives of this thesis is to develop a dynamic model of a permanent magnet synchronous generator (PMSG) wind turbine (WT) using Matlab and conduct some different simulations with wind changes and grid changes also including grid faults to validate the model.

II. Literature review

The introduction of fault-ride through capability it is necessary for reliable and stable operations of utility power grids, where there is high level of penetration of wind turbines.

In the grid faults three major issues are identified: fault detection, the fault ride-through itself and the recovery after the fault. In the past the wind turbines were disconnected from the grid when there was a fault, but nowadays they are designed not to only stay connected and recover fast the power generation after a fault clearance, but also provide voltage support and generate capacitance reactive power. [4]

Fault ride-through has been introduced as one of the most important requirements of grid codes regarding the wind farm operations. The capacity of the generation systems of continuing connected to the grid during and after the fault depends a lot on the technology itself and the design of the generation, as the short circuit levels and the characteristics of the control system.

Countries as Denmark, Ireland, Germany and UK have different requirements of FRT capability depending on the system: transmission system (TS) and distribution system (DS), while the others only focus on the transmission system only.

III. Type 4 wind turbine modelling and control

A. Aerodynamic modelling

The power from a wind turbine at the rotor can be expressed as:

$$P_{\mathrm{t}} = \frac{1}{2} C_{\mathrm{p}}(\lambda) \rho R^2 v^3 \tag{1}$$

where $C_p()$ it corresponds to the power coefficient, which is a representation of the aerodynamic performance of the wind turbine rotor. C_p is function of the blade tip speed ratio as stated by Borowy Bogdan S. and Salameh Ziyad M. 1997:

$$\lambda = \frac{R\omega}{v} \tag{2}$$

There is not a fix $C_p(t)$ curve as is specific for each turbine and it depends particularly in the blade design.

The aerodynamic torque can be expressed as

$$T_{\mathrm{t}} = \frac{P_{\mathrm{t}}}{\omega} = \frac{1}{2} \frac{C_{\mathrm{p}}(\lambda)}{\lambda} \rho \pi R^2 v^2 \tag{3}$$

And the power output at the generator can be expressed as

$$P_{\mathrm{G}} = \frac{1}{2} \nu C_{\mathrm{p}}(\lambda) \rho \pi R^2 v^3 \tag{4}$$

where represents the total efficiency of the mechanical transmission system and the generator.

B. PMSG modelling

. PMSG modelling is not an easy task and it requires, to make some assumptions in order to simplify the model:

- Permanent magnet conductivity is zero
- No field current dynamics
- The saturation is neglected
- EMF is sinusoidal
- Hysteresis losses are negligible

Given the assumptions needed, the PMSG can be modelled as follows in the direct-quadrature (DQ) coordinate system

$$V_{\mathrm{qs}} = -r_{\mathrm{s}} i_{\mathrm{qs}} + L_{\mathrm{qs}} \frac{d}{dt} i_{\mathrm{qs}} - \omega_{\mathrm{r}} L_{\mathrm{ds}} i_{\mathrm{ds}} + \omega_{\mathrm{r}} \frac{dy}{dx} \psi_{\mathrm{ds}} \tag{5}$$

$$V_{\mathrm{ds}} = -r_{\mathrm{s}} i_{\mathrm{ds}} + L_{\mathrm{ds}} \frac{d}{dt} i_{\mathrm{ds}} + \omega_{\mathrm{r}} L_{\mathrm{qs}} i_{\mathrm{qs}} \tag{6}$$

Then, the electromagnetic torque can be expressed as

$$T_{\mathrm{e}} = \frac{3P}{4} [i_{\mathrm{ds}} i_{\mathrm{qs}} (L_{\mathrm{ds}} - L_{\mathrm{qs}}) + i_{\mathrm{qs}} \frac{d}{dt} \psi_{\mathrm{ds}}] \tag{7}$$

where T_e represents the electromagnetic torque in *Nm* and P the pole number at the generator stator. It is possible to obtain the relationship between the angular velocity of the rotor and the mechanical angular velocity of the wind turbine as follows

$$\omega = \frac{2\omega_{\mathrm{r}}}{PG} \tag{8}$$

$$\frac{d}{dt} \omega_{\mathrm{r}} = \frac{P}{2J} (T_{\mathrm{m}} - T_{\mathrm{e}}) \tag{9}$$

The input torque to the generator it can be easily obtained as

$$T_{\mathrm{m}} = \frac{Tt}{G} \tag{10}$$

In case of a PMSG direct-driven wind turbine, as the one studied in this project, *G=1*, and $T_m = T_t$.

1) Inverse Park and Clarke transform: The transformation from the axis reference frame () to the rotating reference frame (*dq*) is called Park transform. The inverse transformation from the 3-phase reference frame to the 2-phase stator axis () is called the Clarke transform.

Inverse Park transform assumes that frame has an angle $_{\text{Field}}$ with the *dq* frame that can be expressed as

$$\begin{bmatrix} \alpha \\ \beta \end{bmatrix} = \begin{bmatrix} cos(\theta_{\text{Field}}) & -sin(\theta_{\text{Field}}) \\ sin(\theta_{\text{Field}}) & sin(\theta_{\text{Field}}) \end{bmatrix} \begin{bmatrix} d \\ q \end{bmatrix} \tag{11}$$

Finally it is possible to obtain the inverse Clarke transform as

$$\begin{bmatrix} V_{\mathrm{a}} \\ V_{\mathrm{b}} \\ V_{\mathrm{c}} \end{bmatrix} = \begin{bmatrix} 1 & 0 \\ -\frac{1}{2} & \frac{\sqrt{3}}{2} \\ -\frac{1}{2} & -\frac{\sqrt{3}}{2} \end{bmatrix} \begin{bmatrix} \alpha \\ \beta \end{bmatrix} \tag{12}$$

2) Matlab modelling: There are many different ways to simulate the curve of the *Cp()*. In order to get the graph an iterative process is needed which can be really complex. In this project, the following polynomial approximation has been used

$$Cp(\lambda) = a1 + a2\lambda + a3\lambda^2 + a4\lambda^3 + a5\lambda^4 + a6\lambda^5 \tag{13}$$

PMSG, can be designed using equations presented before in Section III-B.

Figure shows the model that implements the different transforms from the 3-phase balance frame to the DQ-coordinate system through the Park transform.

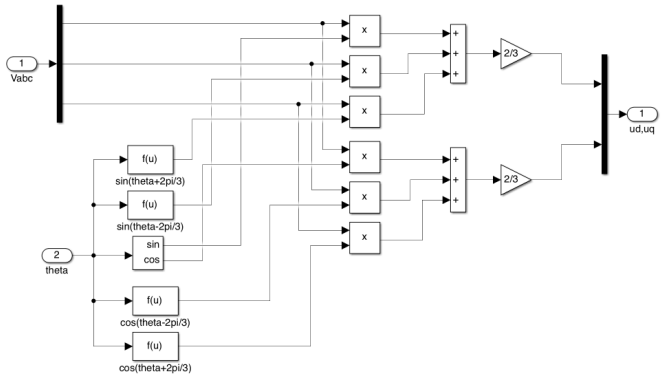

Fig. 1. Model calculation for u_d,u_q

Once the stator voltage in the dq-axis is calculated through Park transform, it is possible to obtain the stator current in the DQ-coordinate system from the equations (5) and (6).

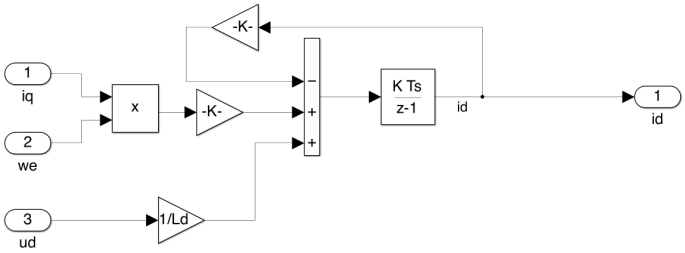

Fig. 2. Simulation model for the current stator

Finally from 7 the electromagnetic torque can be obtained, as it shows the model. Figure 3 shows the transformation of the voltge V_{abc} to u_{dq} reference in order to compute both $i_{d,q}$.

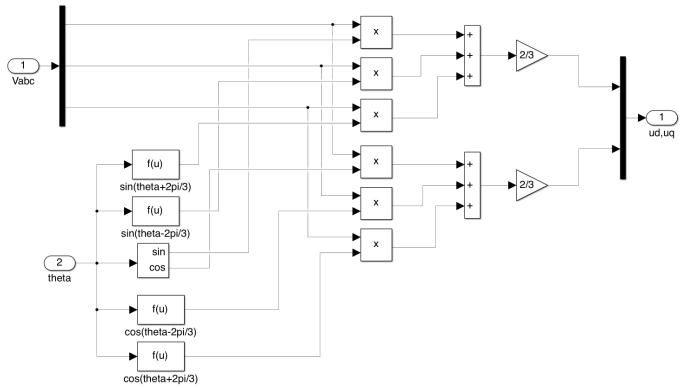

Fig. 3. Voltage transformation from *abc* to *dq* reference.

Figure 4 it is possible to see the model created to compute the current in the axis reference frame.

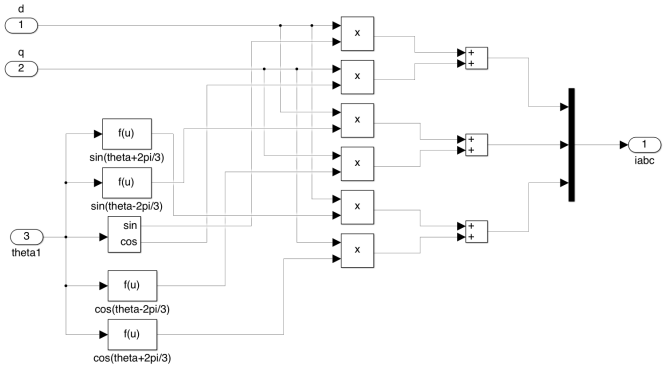

Fig. 4. Current transformation from *dq* to *abc* axis reference.

Once the required previous transformations are done it is possible to compute the current in the rotating reference fram *(dq)* as shows Figure 5 and Figure 6.

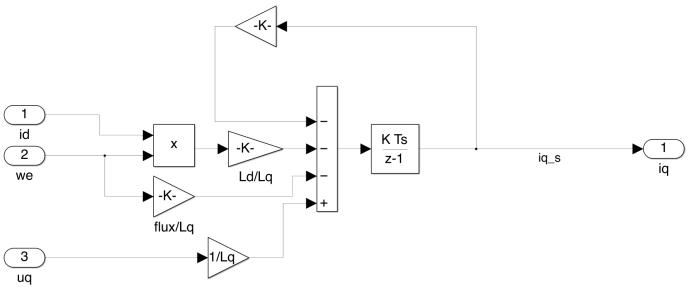

Fig. 5. i_d calculation

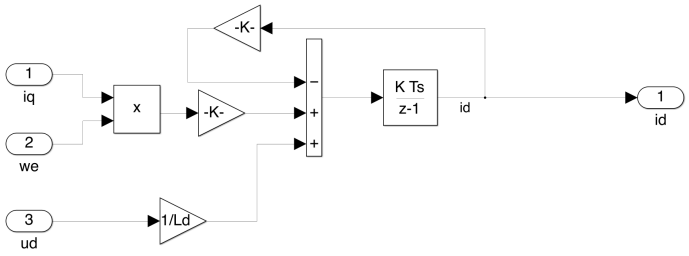

Fig. 6. i_q calculation

C. VSC modelling

In order to simplify the study and control of the VSC the six IGBTs from the original model are replaced by three constant voltage sources as shown in Figure 7.

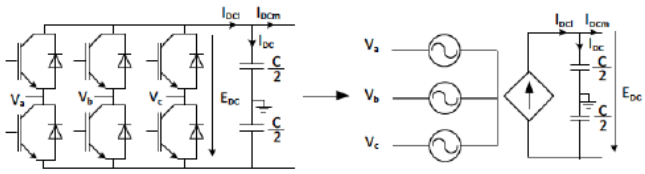

Fig. 7. VSC simplification. [12]

The simplified model splits the converter into two parts: the AC part and the DC part. In the AC part, the converter is modelled as a voltage source, while the DC part is modelled as a current source, as seen in Figure 7. The current source from the DC part reflects the active power exchanged between the AC and the DC part and assures the power balance of the system.

The current from the DC part neglecting the power conversion losses as,

$$I_{\mathrm{DCl}} = \frac{P_{\mathrm{AC}}}{E_{\mathrm{DC}}} \tag{14}$$

Through the voltage equations it is possible to obtain an equivalent scheme of the AC part of the converter in order to simplify the study,

$$\begin{bmatrix} v_{zq} \\ v_{zb} \\ v_{zc} \end{bmatrix} - \begin{bmatrix} v_{la} \\ v_{lb} \\ v_{lc} \end{bmatrix} - (v_{ol} - v_{oz}) \begin{bmatrix} 1 \\ 1 \\ 1 \end{bmatrix} = \begin{bmatrix} r_l & 0 & 0 \\ 0 & r_l & 0 \\ 0 & 0 & r_l \end{bmatrix} \begin{bmatrix} i_a \\ i_b \\ i_c \end{bmatrix} + \begin{bmatrix} l_l & 0 & 0 \\ 0 & l_l & 0 \\ 0 & 0 & l_l \end{bmatrix} \frac{d}{dt} \begin{bmatrix} i_a \\ i_b \\ i_c \end{bmatrix} \tag{15}$$

where,

- v_{za}, v_{zb}, v_{zc}, corresponds to the instant grid voltage on the abc reference
- v_{la}, v_{lb}, v_{lc}, corresponds to the instant converter voltage on the abc reference
- i_a, i_b, i_c, corresponds to the instant current on the abc reference
- v_{lo}-v_{zo}, corresponds to the difference between the converter and the neutral phase of the grid

From this equations the diagram shown on Figure 8 can be extracted.

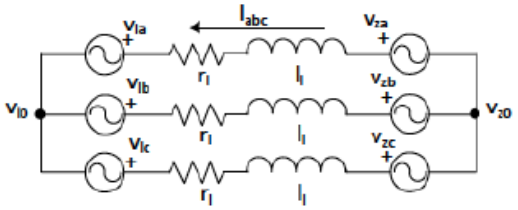

Fig. 8. Equivalent model from the AC part for the VSC. [12]

In cases where there is no neutral phase, it can be extracted that v_{lo}-v_{zo}=0 and the voltage equations can be simplified to

$$\begin{bmatrix} v_{zq} \\ v_{zd} \end{bmatrix} - \begin{bmatrix} v_{lq} \\ v_{ld} \end{bmatrix} = \begin{bmatrix} r_l & l_l\omega_e \\ -l_l\omega_e & r_l \end{bmatrix} \begin{bmatrix} i_q \\ i_d \end{bmatrix} + \begin{bmatrix} l_l & 0 \\ 0 & l_l \end{bmatrix} \frac{d}{dt} \begin{bmatrix} i_q \\ i_d \end{bmatrix} \tag{16}$$

The converter control diagram can be found on Figure 9 , based on a two level control scheme. The internal controller allows tho regulate the AC current in the *qd0* reference, while the external controller allows to regulate the DC voltage in the same reference.

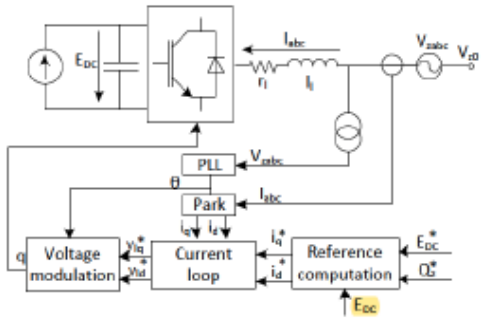

Fig. 9. Control scheme of a VSC for a wind turbine. [12]

As both controllers works on the qd0-reference, through the reference rotation to adjust the electrical angle of the grid. For that reason the Phase Locked Loop (PLL) is required, at it allows the tracking of the grid angle. This angle allows to compute the inverse Park transform, well needed for the system.

D. Current Loop Controller

Current Loop Controller allows to compute the voltage that the VSC needs to apply ($v_{l,q}$ i $v_{l,d}$) to ensure that the current that flows through the converter is the same the reference current of the controller (i^*_q,i^*_d).

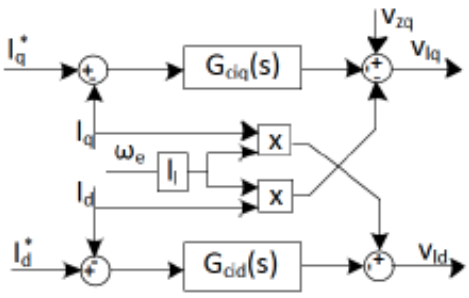

Fig. 10. Current Loop Controller diagram. [12]

If v_{zd}=0 is assumed, the voltage equations can be written as

$$\begin{bmatrix} v_{zq} \\ 0 \end{bmatrix} - \begin{bmatrix} v_{lq} \\ v_{ld} \end{bmatrix} = \begin{bmatrix} r_l & l_l\omega_e \\ -l_l\omega_e & r_l \end{bmatrix} \begin{bmatrix} i_q \\ i_d \end{bmatrix} + \begin{bmatrix} l_l & 0 \\ 0 & l_l \end{bmatrix} \frac{d}{dt} \begin{bmatrix} i_q \\ i_d \end{bmatrix} \quad (17)$$

where it is possible to see the relation between components q and d of the current and voltage, which can be controlled independently.

Decoupling the components q and d of the voltage and integrating them inside the previous equations, the following voltage equations are obtained

$$\begin{bmatrix} v_{lq} \\ v_{ld} \end{bmatrix} = \begin{bmatrix} -\hat{v}_{lq} + v_{zq} - l_l\omega_e i_{ld} \\ -\hat{v}_{ld} + l_l\omega_e i_{lq} \end{bmatrix} \quad (18)$$

The transfer functions between controller and converter can be written as

$$\frac{\hat{v}_{lq}(s)}{i_q(s)} = \frac{1}{l_l s + r_l} \quad (19)$$

$$\frac{\hat{v}_{ld}(s)}{i_d(s)} = \frac{1}{l_l s + r_l} \quad (20)$$

The controller for the previous transfer functions can be designed using the Internal Model Control technique, which allows to obtain the following controller

$$G_{ciq}(s) = G_{cid}(s) = \frac{K_p s + k_i}{s} \quad (21)$$

With the respective constants,

$$K_p = \frac{l_l}{\tau} \quad (22)$$

$$K_i = \frac{r_l}{\tau} \quad (23)$$

Finally, to obtain the i^*_q and i^*_d reference values from active and reactive power (P^*, Q^*), the following power theory is applied,

$$P^* = \frac{3}{2}(v_{zq} i^*_q + v_{zs} i^*_d); Q^* = \frac{3}{2}(v_{zq} i^*_d - v_{zd} i^*_q) \quad (24)$$

As defined before, v_d=0 so i^*_q and i^*_d can be obtained as

$$i^*_q = \frac{2}{3}\frac{P^*}{v_{zq}} \quad (25)$$

$$i^*_d = \frac{2}{3}\frac{Q^*}{v_{zq}} \quad (26)$$

Q^* will be fixed and the active power P^* will adjust in order to regulate the continuous voltage.

E. Voltage Controller

This part allows to obtain the values for P^* and i^*_q as shown in Figure 11.

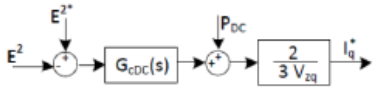

Fig. 11. Voltage Controller diagram. [12]

The PI values can be obtained as,

$$K_{\mathrm{P,DC}} = C\xi_{\mathrm{E}}\omega_{\mathrm{E}} \quad (27)$$

$$K_{\mathrm{iDC}} = \frac{C\omega^2{}_{\mathrm{E}}}{2} \quad (28)$$

where C is the condenser from the dc part of the converter, w_E the desired angular velocity in the voltage loop and ξ_E corresponds to the *damping ratio* of the loop.

F. Phase Locked Loop

Phase Locked Loop (PLL) its a system where the phase and frequency are feedback-able. It is used to determine the angle and angular velocity of the grid. The other objective of this controller is to stabilize v_d to 0, reason why it has been assumed that v_{zd}=0. The general diagram for a PLL is shown in Figure 12 .

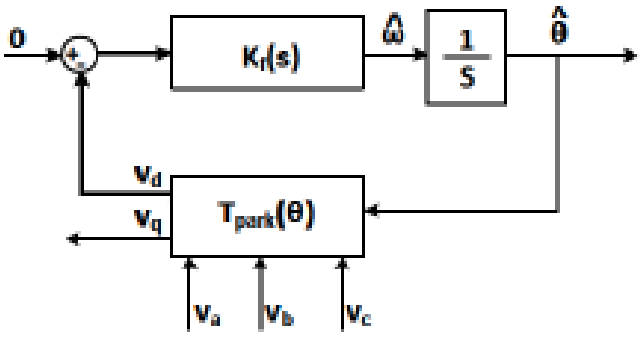

Fig. 12. Voltage Controller diagram. [12]

Through linearization it is possible to obtain the system equations, required to obtain the constant values of the PI controller:

$$K_{\mathrm{f}}(s) = (K_{\mathrm{p,PLL}} + \frac{K_{\mathrm{i,PLL}}}{s}) + w_{\mathrm{e}} \quad (29)$$

$$K_{\mathrm{i,PLL}} = \frac{1}{\tau_{\mathrm{PLL}}} \quad (30)$$

$$w_{\mathrm{e}} = 2\pi f_{\mathrm{e}} \quad (31)$$

G. Fault Ride Through modelling

The FRT response can be divided in different parts. Different strategies are followed for the reactive power and the active power. If a voltage drop occurs, the WT needs to adjust the output power according to the grid code requirements of the country where is installed.

1) Stage 1: ride-through control during a fault: This stage corresponds to the interval between t_1 and t_3. The reactive current i_{qref_F1} is given by

$$i_{\text{qref}_F1}(t) = -[min(i_{\text{lim}_Q}, k(e_{\text{set}} - e_{\text{g}})l_{\text{n}})] + i_{\text{qref0}}] \quad (32)$$

where i_{qref0} is the reactive current reference before the fault. In the case of the active current, $i_{dref_F1}$is expressed by

$$i_{\text{dref}_F1}(t) = (\min(i_{\text{drefN}}, \sqrt{i^2_{\text{max}} - i^2_{\text{qrefF1}}}) = min[(k_{\text{Pudc}}(u_{\text{dcref}} - u_{\text{dc}}) + k_{\text{Iudc}} \int (u_{\text{dcref}} - u_{\text{dc}})dt, \sqrt{i^2_{\text{max}} - i^2_{\text{qrefF1}}}] \quad (33)$$

2) Stage 2: Post fault recovery control: This stage occurs between t_3 and t_7 and the voltage approximately return to the prefault value. In this stage the control differs between active power and reactive power:

- **Active current reference:** Based on,

$$P_{\text{F1}} = 1.5e_{\text{d}}i_{\text{d}}Q_{\text{F1}} = -1.5e_{\text{d}}i_{\text{q}} \quad (34)$$

where e_d is the active power, i_d and i_q the respective active and reactive power.And,

$$P_{\text{F2-1}}(t) = P(t_3) \quad (35)$$

where $P(t_3)$ is the active power at t_3, the active current reference $i_{\text{drefF2-1}}$ at Stage 2-1 can be obtained as,

$$i_{\text{dref-F2-1}}(t) = P(t_3)/(1.5e_{\text{d}}) \quad (36)$$

At Stage 2-2, the current reference $i_{\text{drefF2-2}}$ can be obtained as,

$$i_{\text{dref-F2-2}}(t) = r_{\text{id}}(t\text{-}t_4) + P(t_4)/(1.5e_{\text{d}}), \text{ when } P(t_4) \text{¡} P_0 i_{\text{dref0}}, \text{ when } P(t_4) = P_0 \quad (37)$$

where r_{id} corresponds to the active current recovery rate and i_{dref0} corresponds to the previous active current reference.

- **Reactive current reference:** Similar to active current reference, the reference current for the reactive reference will be derived differently depending on each sub stage of the post fault recovery control. During Stage 2-1, the WT keeps supplying reactive power, so its value $i_{qrefF2\text{-}1}$ can be derived as:

$$i_{\text{qref-F2-1}}(t) = -[\min(i_{\text{limQ}}, k(e_{\text{set}}\text{-}e_{\text{g}})l_{\text{n}})], \text{ scheme } 1 \max(Q(t_3), 0)/(-1.5e_{\text{d}}), \text{ scheme } 2 \quad (38)$$

In Stage 2-2, the control strategy follows the reactive power outer loop control, so the $i_{qrefF2\text{-}2}$ can be expressed as,

$$i_{\text{qref-F2-2}}(t) = r_{\text{iq}}(t\text{-}t_5) + Q(t_5)/(-1.5e_{\text{d}}), \text{ when } Q(t_5) \neq Q_0 i_{\text{qref0}}, when Q(t_5) = Q_0 \quad (39)$$

where r_{iq} corresponds to the reactive current recovery rate.

For the FRT control its important to identify the following parameters:

- k, corresponds to the reactive power support coefficient which can be calculated under a small voltage dip as:

$$k = (i_{\text{qM0}} - i_{\text{qM}})/[I_{\text{n}}x(e_{\text{set}} - e_{\text{g}})] \quad (40)$$

where i_{qM0} corresponds to the reactive current measurement previous to the fault.

- r_{id}, corresponds to the active current recovery rate which can be calculated under severe voltage dips, and it can be calculated as:

$$r_{\text{id}} = [i_{\text{dM}}(t_7) - i_{\text{dM}}(t_4)]/(t_7 - t_4) \quad (41)$$

where $i_{dM}(t_x)$ corresponds to the measured active power at t_x.

- r_{iq}, corresponds to the reactive current recovery rate which can be calculated from real data after the post-fault period, and it can be calculated as:

$$r_{\text{iq}} = [i_{\text{qM}}(t_6) - i_{\text{qM}}(t_5)]/(t_6 - t_5) \quad (42)$$

where $i_{qM}(t_x)$ corresponds to the measured reactive power at t_x.

IV. MODEL VALIDATION AND RESULTS

The chosen wind turbine is a 1.5MW type-4 WT, which has the parameters shown in Table I.

Parameters	Values	Parameters	Values
Rotor diameter	66 m	Generator rated power	1.58 MVA
Cut-in wind speed	3 m/s	Generator rated voltage	0.62 kV
Cut-out wind speed	22 m/s	Generator rated current	1.45 kA
Rated wind speed	12 m/s	Generator frequency	12.69 Hz
DC-link voltage	1.1 kV	Pole pairs	56
Transformer rated capacity	1.6 MVA	Stator resistance	4.35m
Direct-axis inductance	1.6 mH	Quadrature-axis inductance	1.6 mH

TABLE I
WT PARAMETERS FOR 1.5 MW TYPE-4 WT. [14]

For the design of the VSC the parameters that have been used can be found in Table II. The spanish grid code have been used. [15].

The requirements are shown in Figure 13 . While the turbine is above the curve, the WT has to stay connected to the grid. In the spanish grid code, turbines has to provide reactive power to support the voltage.

Parameters	Controller parameters				
	Current Loop		Voltage controller		PLL
	k_p	k_i	k_p	k_i	k_p
Values	5.4	500	0.302	89.48	1

TABLE II
PI PARAMETERS FOR THE VSC CONTROLLER. [12]

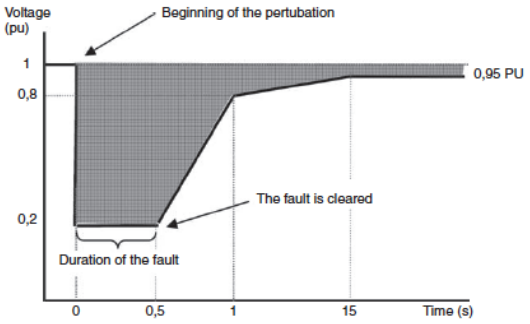

Fig. 13. Grid code requirements in Spain [16].

Using the turbine parameters from [17] as base the following power curve is obtained:

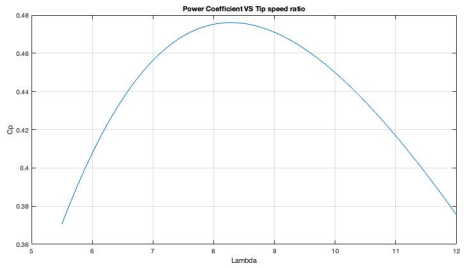

Fig. 14. C_p curve for the modelled turbine

The obtained curve shows that maximum C_p is almost at 0.475, which corresponds to the value from [17]. The next step is to simulate the PMSG model. The same turbine from [17] is being used which has a nominal torque of $_t^N$ =0.322e6 Nm. From the PMSG Matlab model the following curve can be obtained.

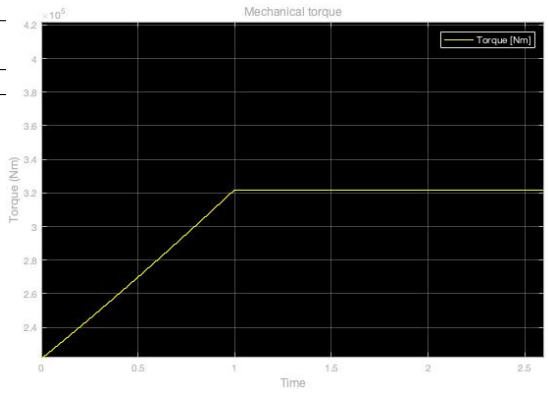

Fig. 15. Simulated PMSG turbine under nominal conditions.

As Figure 15 shows, once the nominal velocity is achieved, the nominal torque is achieved as expected.

One of the objectives of this thesis is to control the turbine in front of changes in the wind speed and parameters of the turbine. This simulations is carried out in order to see how the different parameters of the voltage source converter works and see if the turbine is stabilized and works correctly.

Figure 16,shows that as the power generated in the wind turbine changes from 1MW to 1.5MW at t=1s the current i_q is able to stabilize in less than 1s to its current reference value.

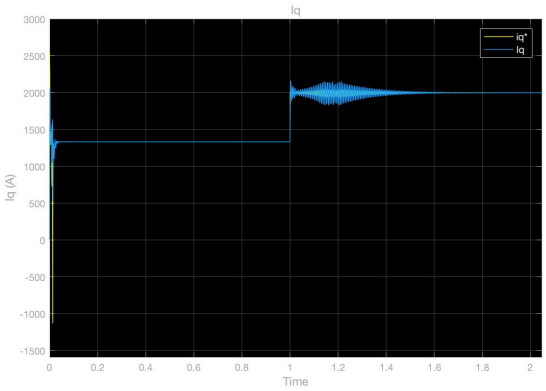

Fig. 16. i_q simulation for wind speed changes.

Detail of the previous figure is shown in Figure 17 , where the system tries to return to the 98% of its value after $4_{\text{control-loop}}$, where $_{\text{control-loop}}$=0.1s. That behaviour shows a good control of the control loop as it is able to stabilize the system with the speed that is requested.

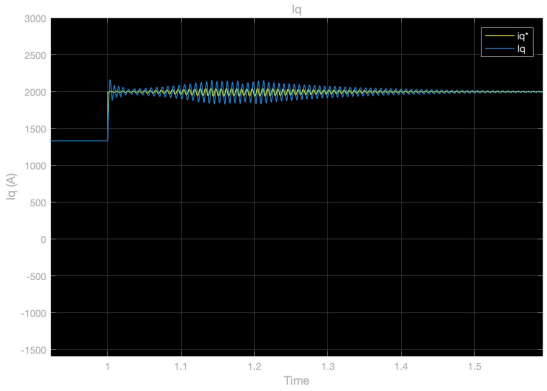

Fig. 17. i_q detail simulation for wind speed changes.

In the reality, the wind turbine won't suffer this sudden changes in speed so the stabilization will be more smooth, it is true that wind speed changes a lot, but never as a step (what it has been used in order to simulate it).

Following the control principle of the VSC the reactive power is fixed to a desired value [12] and the active power P^* fluctuates in order to regulate the continuous voltage.

For the i_d the following behaviour is obtained as seen in Figure 18.

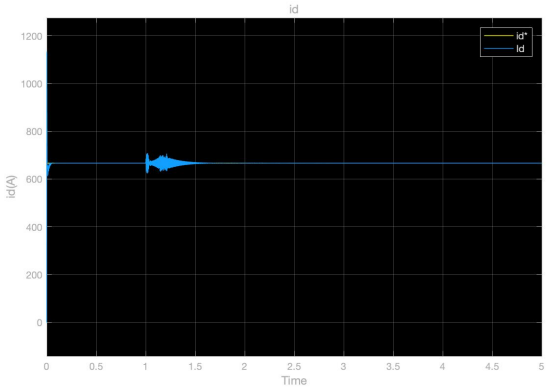

Fig. 18. i_d simulation for wind speed changes.

The fluctuation on the real value of i_d is due to the changes in the active power, but as the reactive power is constant it returns to the same reference value as before. Figure 19 shows the detail of this fluctuation and how in a similar way of i_q it returns to the 98% of its value in $4_{\text{control-loop}}$.

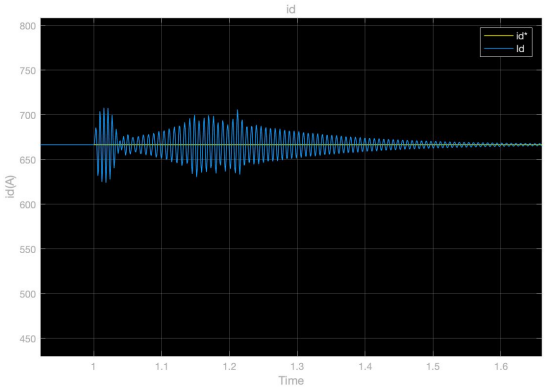

Fig. 19. i_d detailed simulation for wind speed changes.

The next and final step is to simulate a grid fault and check the behaviour of the full model. For this case, the parameters that have been used are the ones from Table I and Table II as solid studies are available to validate the results of this thesis.

This part requires the design of a fault which will be applied to the machine side for the sake of simplicity as seen in Figure 20.

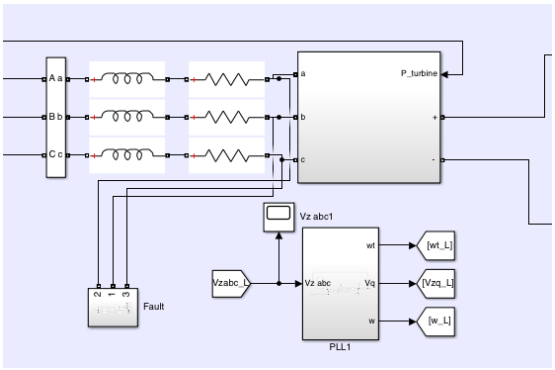

Fig. 20. Fault implementation to the machine side.

The fault has been implemented as impedance connected to the ground with a switch (Figure 21) in order to simulate the fault at specific time.

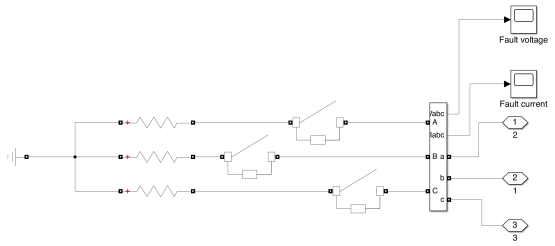

Fig. 21. Fault detail.

As seen in Figure 22 , a fault occurs at t=2s and the current

flows through the fault.

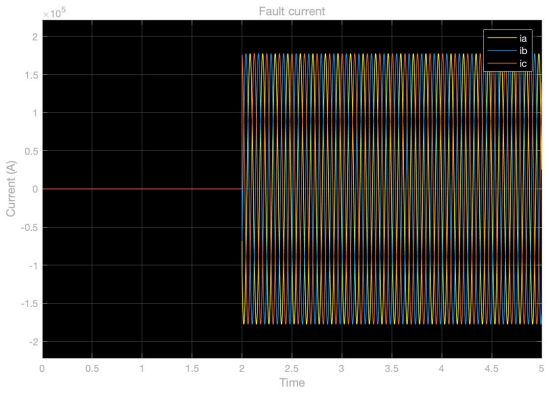

Fig. 22. Current flow through fault branch.

As exposed in chapter 3, there are different stages on the FRT control methodology, which can be easily a project by itself. As this project focuses in the general modelling and control of the WT, only Stage 1 has been tested and refined, even though all of the different stages have been designed.

Figure 23, shows that when the fault occurs at t=2s all the current of the machine side is affected.

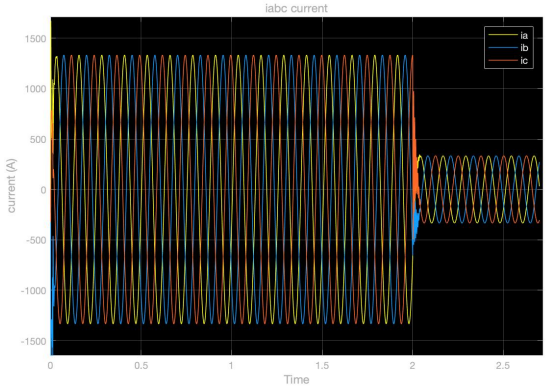

Fig. 23. MCS current when the fault occurs at t=2s.

Studying in detail the different currents of the converter, it is possible to see that i_q follows the equations exposed previously of Stage 1, the reactive current adjusts itself as exposed

$$i_{\text{qref}_F1}(t) = -[min(i_{\text{lim}_Q}, k(e_{\text{set}} - e_{\text{g}})l_{\text{n}})] + i_{\text{qref0}} \qquad (43)$$

In Figure 24,the reactive current decreases and is able to see to its new reference post fault, following the same principle of stabilization than the one exposed for the full VSC modelling.

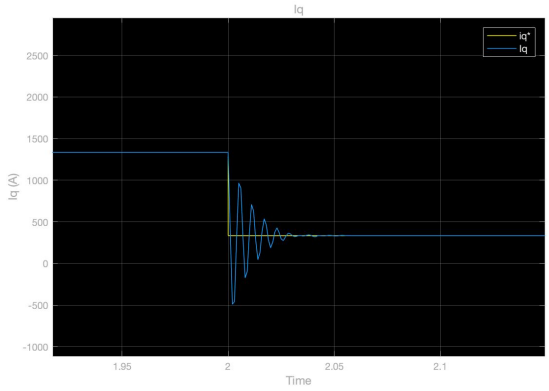

Fig. 24. Reactive current at t=2s

This project covers different topics of the engineering design of a WT, from the aerodynamic part to the dynamic analysis part. The study of the whole system of the turbine has shown that even the most abrupt changes on a WT, which is its normal operation every day, can be overwhelmed with a good control design.

Figure 14 has shown that with a good iterative code process is possible to adjust the simulated power curve to the theoretical one given from the literature review. Once that was done, the PMSG model was tested to see if the dynamic model was able to achieve the desired torque and power when wind changes where happening.

Even the changes in wind speed weren't as real as expected, the generator model achieves the expected results as seen in Figure 15.

The basic modelling has been able to reproduce quite exactly the theoretical results for the studied wind turbine, as it doesn't require much parameters adjustment.

Once the control part has been tested the results have changed a little. VSC modelling and FRT modelling requires to adjust the different parameters of the PIs of the different control loops.

Full VSC modelling request a lot of design and parameter changes and given the case study has complicated a lot the control. Even that, as seen in Figure 16, Figure 17Figure 18, Figure 19 the controller is able to achieve the reference value of the currents in the requested time for which was designed.

Finally, for the FRT control it was necessary to simplify the scope of the controller as it requires a lot of time to design and test the correct behaviour of it. As some literature explains [18], [19], [20] an iterative process is required to adjust the correct parameters. In order to being able to deliver a decent project in the global scope, this process have been reduced to the post fault control.

As seen in Figure 23 and 24 the system is able become stable after the fault and not destabilizing.

A. Future work

Following what it was said on the previous section, this project ca be easily enlarge in something more complex. The future work to be done is the following:

- Create an realistic daily wind profile and simulate all the different parts with it.
- For the VSC converter, even it has a good response the parameters can be adjusted in order to get more smooth control
- For the FRT control, the different stages can be adjusted and improved to being able to support all the fault process.
- As this have been applied to only one offshore WT, the study can be increased to a farm level including different wind turbines with different faults at different times and see how the whole cluster of turbines behaves.

REFERENCES

[1] "OFFSHORE WIND IN EUROPE." [ONLINE]. AVAILABLE: WWW.WINDEUROPE.ORG

[2] G. VENKATARAMANAN AND C. MARNAY, "A LARGER ROLE FOR MICROGRIDS," *IEEE Power and Energy Magazine*, VOL. 6, NO. 3, 2008, DOI: 10.1109/MPE.2008.918720.

[3] B. KROPOSKI, R. LASSETER, T. ISE, S. MOROZUMI, S. PAPATHANASSIOU, AND N. HATZIARGYRIOU, "MAKING MICROGRIDS WORK," *IEEE Power and Energy Magazine*, VOL. 6, NO. 3, 2008, DOI: 10.1109/MPE.2008.918718.

[4] I. ERLICH, W. WINTER, AND A. DITTRICH, "ADVANCED GRID REQUIREMENTS FOR THE INTEGRATION OF WIND TURBINES INTO THE GERMAN TRANSMISSION SYSTEM," 2006. DOI: 10.1109/PES.2006.1709340.

[5] A. D. HANSEN ET AL., "MAPPING OF GRID FAULTS AND GRID CODES - RISØ-R-1617(EN)," *IEEE Transactions on Energy Conversion*, VOL. 35, NO. 3, 2008.

[6] M. NASIRI AND R. MOHAMMADI, "PEAK CURRENT LIMITATION FOR GRID SIDE INVERTER BY LIMITED ACTIVE POWER IN PMSG-BASED WIND TURBINES DURING DIFFERENT GRID FAULTS," *IEEE Trans Sustain Energy*, VOL. 8, NO. 1, 2017, DOI: 10.1109/TSTE.2016.2578042.

[7] D. M. YEHIA, D. E. A. MANSOUR, AND W. YUAN, "FAULT RIDE-THROUGH ENHANCEMENT OF PMSG WIND TURBINES WITH DC MICROGRIDS USING RESISTIVE-TYPE SFCL," *IEEE Transactions on Applied Superconductivity*, VOL. 28, NO. 4, 2018, DOI: 10.1109/TASC.2018.2821362.

[8] M. NASIRI, J. MILIMONFARED, AND S. H. FATHI, "A REVIEW OF LOW-VOLTAGE RIDE-THROUGH ENHANCEMENT METHODS FOR PERMANENT MAGNET SYNCHRONOUS GENERATOR BASED WIND TURBINES," *Renewable and Sustainable Energy Reviews*, VOL. 47. 2015. DOI: 10.1016/J.RSER.2015.03.079.

[9] J. F. CONROY AND R. WATSON, "LOW-VOLTAGE RIDE-THROUGH OF A FULL CONVERTER WIND TURBINE WITH PERMANENT MAGNET GENERATOR," *IET Renewable Power Generation*, VOL. 1, NO. 3, 2007, DOI: 10.1049/IET-RPG:20070033.

[10] A. GENCER, "ANALYSIS AND CONTROL OF FAULT RIDE THROUGH CAPABILITY IMPROVEMENT PMSG BASED ON WECS USING ACTIVE CROWBAR SYSTEM DURING DIFFERENT FAULT CONDITIONS," *Elektronika ir Elektrotechnika*, VOL. 24, NO. 2, 2018, DOI: 10.5755/J01.EIE.24.2.20637.

[11] M. R. ISLAM ET AL., "FAULT RIDE THROUGH CAPABILITY IMPROVEMENT OF DFIG BASED WIND FARM USING NONLINEAR CONTROLLER BASED BRIDGE-TYPE FLUX COUPLING NON-SUPERCONDUCTING FAULT CURRENT LIMITER," *Energies (Basel)*, VOL. 13, NO. 7, 2020, DOI: 10.3390/EN13071696.

[12] A. EGEA-ALVAREZ, A. JUNYENT-FERRÉ, AND O. GOMIS-BELLMUNT, "ACTIVE AND REACTIVE POWER CONTROL OF GRID CONNECTED DISTRIBUTED GENERATION SYSTEMS," *Green Energy and Technology*, VOL. 96, 2012, DOI: 10.1007/978-3-642-22904-63.

[13] K. E. OKEDU, "IMPROVING THE PERFORMANCE OF PMSG WIND TURBINES DURING GRID FAULT CONSIDERING DIFFERENT STRATEGIES OF FAULT CURRENT LIMITERS," *Front Energy Res*, VOL. 10, JUN. 2022, DOI: 10.3389/FENRG.2022.909044.

[14] J. G. SLOOTWEG AND W. L. KLING, "MODELLING WIND TURBINES FOR POWER SYSTEM DYNAMICS SIMULATIONS: AN OVERVIEW," *Wind Engineering*, VOL. 28, NO. 1 SPEC. ISS. 2004. DOI: 10.1260/0309524041210801.

[15] YUANZHANG SUN, "MODELING AND MODERN CONTROL OF WIND POWER". 2018. DOI: 10.1002/9781119236382

[16] MINISTERIO DE INDUSTRIA DE ESPAÑA, "PO 12.3. REQUISITOS DE RESPUESTA FRENTE A HUECOS DE TENSIÓN DE LAS INSTALACIONES EÓLICAS," *Boe*, VOL. 254, 2006.

[17] A. JUNYENT-FERRÉ, "CONTROL OF POWER ELECTRONIC CONVERTERS FOR THE OPERATION OF WIND GENERATION SYSTEMS UNDER GRID DISTURBANCES," 2011.

[18] J. QI, W. LI, P. CHAO, X. LIANG, Y. SUN, AND Z. LI, "GENERIC EMT MODELING METHOD OF TYPE-4 WIND TURBINE GENERATORS BASED ON DETAILED FRT STUDIES," *Renew Energy*, VOL. 178, 2021, DOI: 10.1016/J.RENENE.2021.06.057.

[19] A. GENCER, "ANALYSIS AND CONTROL OF FAULT RIDE-THROUGH CAPABILITY IMPROVEMENT FOR WIND TURBINE BASED ON A PERMANENT MAGNET SYNCHRONOUS GENERATOR USING AN INTERVAL TYPE-2 FUZZY LOGIC SYSTEM," *Energies (Basel)*, VOL. 12, NO. 12, 2019, DOI: 10.3390/EN12122289

[20] X. YAN, L. YANG, AND T. LI, "THE LVRT CONTROL SCHEME FOR PMSG-BASED WIND TURBINE GENERATOR BASED ON THE COORDINATED CONTROL OF ROTOR OVERSPEED AND SUPERCAPACITOR ENERGY STORAGE," *Energies (Basel)*, VOL. 14, NO. 2, JAN. 2021, DOI: 10.3390/EN14020518.E